Isothermal Curing of Acetylene Functionalized Liquid Crystalline Thermoset Monomers

Arthur J. Gavrin[†] and Elliot P. Douglas*

Department of Materials Science and Engineering, University of Florida, P.O. Box 116400, Gainesville, Florida 32611

Received October 31, 2000; Revised Manuscript Received June 10, 2001

ABSTRACT: To investigate the effects of molecular architecture on the liquid crystalline phases and times to gelation during isothermal curing, two homologous series of acetylene functionalized thermotropic liquid crystalline monomers were synthesized and examined. New liquid crystalline phase−time−temperature−physical transformation diagrams (LCPTTT) were constructed for four of the monomers and illustrate that the monomers change from nematic liquids to isotropic or biphasic gels during isothermal curing. However, reemergence of an ordered phase occurred if the monomers were cured at low enough temperature. The critical temperature for ordered phase retention in the final vitrified material is inversely proportional to the length of the terminal flexible chain. The time to gelation for a single set of isothermal cure conditions did show an increase in gel times with increasing chain length; however, an odd−even effect was seen in both series rather than a linear increase.

Introduction

A number of studies have shown how curing of liquid crystalline thermosets (LCTs) affects the liquid crystalline phases that exist. Often, LCT monomers that are isothermally cured in an isotropic phase (either above the clearing temperature or with nonliquid crystalline monomers) may develop liquid crystalline order during curing. The emergence of liquid crystalline order during cure has been seen in epoxies,[1,2] bis(acetylene)s,[3] bis(cyanoester)s,[4] bis(nadimide)s,[5] and bis(methylnadimide)s.[6] The formation of liquid crystalline order is attributed to chain extension leading to larger molecular aspect ratios. There is also an example of an acetylene functionalized, liquid crystalline monomer isothermally cured in the isotropic phase that regains nematic liquid crystalline order but then converts back to an isotropic phase as curing continues. The initial conversion to nematic is attributed to chain extension; however, the conversion back to the isotropic phase has not yet been completely explained.[5]

A time−temperature−physical transformation (TTT) diagram allows the prediction of a material's physical phase for many different isothermal cure profiles and is a powerful tool for determining, and predicting, processing conditions. TTT diagrams are constructed to relate the time to a transformation, such as gelation or vitrification, to the isothermal cure temperature. Since during a nonisothermal cure cycle a material can undergo various changes similar to those encountered during an isothermal cure cycle, continuous heating transformation (CHT) diagrams have been constructed to display the times and temperatures that these events occur at for various heating rates. An S-shaped line typically represents the devitrification−vitrification−devitrification contour calculated during curing. Many studies of thermosetting systems have calculated physical transformation TTT[6−14] or CHT[6,10−12,15] diagrams to help explain the physical transformations the curing system undergoes during a cure profile. All of these systems are nonliquid crystalline thermosetting materials, thus yielding only physical transformations.

For LCTs, nonequilibrium phase diagrams,[3,5,15] liquid crystalline phase time−temperature−phase transformation diagrams,[1] and process characterization diagrams[16] have been theorized and experimentally constructed. Nonequilibrium phase diagrams illustrate the liquid crystalline phases for a LCT. These phases are noted on a plot of isothermal cure temperature vs the extent of reaction. The physical phases are noted as liquid and solid but do not include information about phase transformations, such as gelation. Lin et al.[1] have constructed a liquid crystalline phase time−temperature−phase transformation diagram for a liquid crystalline epoxy system describing the liquid crystalline phase, and the time to reach that phase, for an isothermal cure profile. Liquid crystalline phase time−temperature−phase transformation diagrams plot the cure temperature vs time rather than extent of reaction. In that diagram, the S-curve represents the time the material must cure to reach the critical chain length for liquid crystallinity by chain extension. This yields similar data to that of the nonequilibrium phase diagram but tells nothing about the physical state of the material. The process characterization diagram is not a phase diagram and does not allow prediction of isothermal cure profiles for the LCT. These diagrams also do not describe the physical phases of the material. Another experimentally determined transformation diagram, relating transformation temperature with cure time for an isothermal cure,[3] has been constructed for a propargyl LCT monomer. The major disadvantage of this type of transformation diagram is that the diagram is based on multiple cure times and only one cure temperature. This means that predictions of the physical phases (or liquid crystalline phases) of the material for different cure temperatures cannot be made.

Thus, while there have been a variety of diagrams constructed to illustrate changes a material undergoes during isothermal curing, they are too limited for

[†] Current address: Polymer Science and Engineering Department, University of Massachusetts, Amherst, MA 01003.

* To whom correspondence should be sent: e-mail edoug@mse.ufl.edu.

10.1021/ma001884+ CCC: $20.00
Published on Web 07/20/2001

practical processing use. Traditional transformation diagrams for nonliquid crystalline materials are limited in the information they are able to display. These diagrams offer information about physical transformations during curing but are not equipped to convey the morphological information needed for liquid crystalline materials. Other experimentally derived transition diagrams for liquid crystalline materials lack the physical information needed during isothermal processing, like gelation.

Gelation and vitrification occur during the curing of thermosetting materials. Gelation corresponds to the formation of an infinite network of cross-linked polymer molecules, while vitrification is defined as the point at which the T_g of the material is equal to the temperature at which the material is being examined. Vitrification marks the transformation from a rubber to a gelled glass if gelation has occurred. Identification of the gel point is important for the processing of thermosetting materials since it represents the highest conversion at which the material can still flow.[17]

A variety of methods and criteria have been established for the determination of both gelation and vitrification. Differential scanning calorimetry (DSC), thermal mechanical analysis (TMA), torsional braid analysis (TBA), viscosimetry, rheometry, thermal scanning rheometry (TSR), and dynamic mechanical thermal analysis (DMTA) are a few of the techniques used to determine physical transformations of curing systems.[7−9,17−21] Although all of these methods have been used to construct transformation diagrams, for historical and practical reasons only TBA and rheologically based techniques are reviewed below.

Many different criteria have been utilized to determine gel points. For rheological testing, multiple criteria have been established. Laza et al.[18] cite four different criteria:

(1) Criterion of maximum peak in tan δ, based on the point where there is a maximum difference between the elastic and viscous behavior of the system.

(2) Criterion corresponding to the crossover between the G' and G'' curves; at this point, the system presents not only an elastic but also viscous behavior as well, storing a similar amount of energy to the energy dissipated.

(3) Criterion of the tangent line to the G' curve; this point corresponds to the crossing between the baseline ($G' = 0$) and the tangent drawn at G' curve when G' reaches a value close to 100 kPa.

(4) Criterion of the viscosity; at this point the real dynamic viscosity η' reaches several determined values (1000, 2000, and 5000 Pa·s).

Another example of a gel point criterion used is by Hong and Chung.[9] They measured the viscosity of vinyl ester resins at various temperatures with a steady shear rate of 9.3 s^{-1} and determined the gelation time "as the time when the viscosity increased very rapidly toward an infinite value". For torsional braid analysis, gelation is determined from a peak in the logarithmic decrement curve.

Our goal for this study is to synthesize a new family of LCTs with flexible tails of various lengths and different mesogenic units, thus providing an opportunity to understand how molecular architecture affects liquid crystalline phase transformations and physical transformations during cure. The monomers studied are similar to ones reported previously by Douglas et al.[3] However, unlike the biphenyl and hydroquinone monomers of the bis(acetylene)s, the monomers presented here do melt and display liquid crystalline phases. To achieve this goal, we construct new liquid crystalline phase−time−temperature−transformation (LCPTTT) diagrams and use these diagrams to help elucidate the effects of molecular architecture on the various transformations. The thermal polymerization of these monomers is believed to proceed by a free-radical addition reaction between ethynyl units to generate a polyene network.[22−24] Trimerization to benzenoid rings is expected to be minimal due to the bulkiness of the flexible chains and the mesogenic unit.

Experimental Section

Materials. All chemicals were used as received. Methyl-4-iodobenzoate, bis(triphenylphosphine)palladium(II) chloride, triphenylphosphine, copper(I) iodide (98%), triethylamine, oxalyl chloride, sodium hydroxide, concentrated hydrochloric acid, diethyl ether, dimethylformamide, methanol, benzene, 1-pentyne (99%), 1-octyne (99%), and biphenol (97%) were all received from Acros Chemical Co. The hydroquinone (99%), 1-hexyne (97%), 1-heptyne (98%), 1-nonyne (99%), and 1-decyne (98%) were received from Aldrich Chemical Co.

General Procedures. Elemental analyses were determined at the Chemistry Department at the University of Florida. ^{1}H NMR (300 MHz) and ^{13}C NMR (75 MHz) were recorded on a Gemini-300 instrument in $CDCl_3$ using TMS as an internal standard.

Synthesis. All of the monomers were synthesized in a similar manner. The nomenclature used for the monomers consists of a number, representing the number of carbons in the flexible chain, followed by either HQ or BP, identifying whether hydroquinone or biphenol was used to form the central unit of the mesogen. The synthesis of the 6BP monomer will be illustrated as an example. Figure 1 shows the synthetic scheme for the LCTs in these series.

p-(1-Octynyl)benzoic Acid (6acid). To a heat/vacuum-dried and argon-flushed 500 mL three-neck flask with stir bar, methyl-4-iodobenzoate (25.7959 g, 0.098 mol), octyne (22.4 mL, 16.231 g, 0.147 mol), triethylamine (250 mL, 181.50 g, 1.794 mol), triphenylphosphine (0.1046 g, 0.3.98 mmol), bis(triphenylphosphine)palladium(II) chloride (0.0979 g, 0.139 mmol), and copper iodide (0.0666 g, 0.3.5 mmol) were added and stirred in an argon atmosphere. The light yellow slurry was stirred under argon for 48 h at room temperature. [Note: times and temperatures varied for different compounds. See specific compound below for details.] The solution was then filtered, and the solid was washed with diethyl ether until light gray or white in color. The yellow filtrate was then reduced under vacuum. The filtrate was then diluted with hexanes and thrice stirred with *n*-alumina gel for 2 h. The alumina gel slurry was filtered and washed with hexanes each time. The filtrate was then reduced under vacuum at room temperature to remove the hexanes. The light yellow liquid was then refluxed with sodium hydroxide (10.8 g, 0.270 mol), water (128 mL), and methanol (140 mL) for 20 h. [For alkynes with shorter chains, the methyl-4-(1-alkynyl)benzoate is a crystal with a melting temperature near room temperature.] The orange liquid was then allowed to cool to room temperature. The solution was then acidified with 37% HCl. A yellow/beige solid formed upon acidification. The solid was then recrystallized twice from hexanes and dried in a vacuum oven at 60 °C for 24 h to yield 15.3202 g (68%) of 6acid. EA: Theory: 78.23% C, 7.88% H, 13.89% O; Actual: 78.52% C, 8.00% H. 300 MHz ^{1}H NMR ($CDCl_3$): δ = 0.89 (t, 3 H, $-CH_3$), 1.4 (m, 6 H, $-CH_2-$), 1.6 (m, 2 H, $-CH_2-$), 2.4 (t, 2 H, $-CH_2-$), 7.4 (d, 2 H, aromatic), 8.0 (d, 2 H, aromatic). 75 MHz ^{13}C NMR ($CDCl_3$): δ = 14.0 ($-CH_3$), 19.5 ($-CH_2-$), 22.6 ($-CH_2-$), 28.5 ($-CH_2-$), 28.6 ($-CH_2-$), 31.3 ($-CH_2-$), 80.1 (acetylene), 94.7 (acetylene), 127.9, 130.0, 131.6 (aromatic), 171.8 ($-COO-$).

p-(1-Pentynyl)benzoic Acid (3acid). Yield 4.19 g (45.5%). EA: Theory: 76.57% C, 6.43% H, 17.00% O; Actual: 76.44%

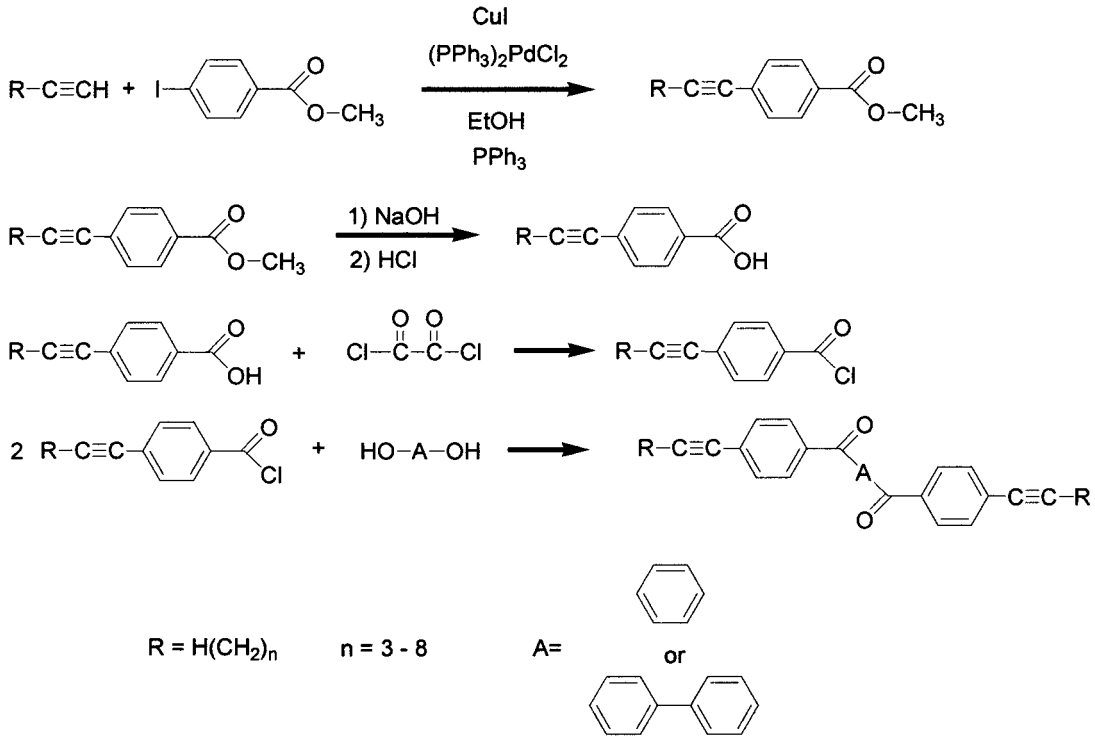

Figure 1. Synthetic scheme of LCT monomers.

C, 6.71% H. 300 MHz ^{1}H NMR ($CDCl_3$): $\delta = 1.0$ (t, 3 H, $-CH_3$), 1.6 (m, 2 H, $-CH_2-$), 2.4 (t, 2 H, $-CH_2-$), 7.5 (d, 2 H, aromatic), 8.0 (d, 2 H, aromatic). 75 MHz ^{13}C NMR ($CDCl_3$): $\delta = 13.5$ ($-CH_3$), 21.5 ($-CH_2-$), 22.0 ($-CH_2-$), 80.2 (acetylene), 94.4 (acetylene), 127.9, 129.9, 130.0, 131.5 (aromatic), 172.0 ($-COO-$).

p-(1-Hexynyl)benzoic Acid (4acid). Yield 16.2728 g (78%). EA: Theory: 77.20% C, 6.98% H, 15.82% O; Actual: 77.35% C, 7.33% H. 300 MHz ^{1}H NMR ($CDCl_3$): $\delta = 0.94$ (t, 3 H, $-CH_3$), 1.4 (m, 2 H, $-CH_2-$), 1.6 (m, 2 H, $-CH_2-$), 2.4 (t, 2 H, CH_2), 7.4 (d, 2 H, aromatic), 8.0 (d, 2 H, aromatic). 75 MHz ^{13}C NMR ($CDCl_3$): $\delta = 13.6$ ($-CH_3$), 19.2 ($-CH_2-$), 22.0 ($-CH_2-$), 30.6 ($-CH_2-$), 80.1 (acetylene), 94.6 (acetylene), 127.9, 130.0, 131.6, (aromatic), 171.9 ($-COO-$).

p-(1-Heptynyl)benzoic Acid (5acid). Yield 14.5425 g (68%). EA: Theory: 77.75% C, 7.46% H, 14.80% O; Actual: 77.49% C, 8.33% H. 300 MHz ^{1}H NMR ($CDCl_3$): $\delta = 0.91$ (t, 3 H, $-CH_3$), 1.4 (m, 4 H, $-CH_2-$), 1.6 (m, 2 H, $-CH_2-$), 2.4 (t, 2 H, $-CH_2-$), 7.4 (d, 2 H, aromatic), 8.0 (d, 2 H, aromatic). 75 MHz ^{13}C NMR ($CDCl_3$): $\delta = 14.0$ ($-CH_3$), 19.5 ($-CH_2-$), 22.2 ($-CH_2-$), 28.3 ($-CH_2-$), 31.1 ($-CH_2-$), 80.0 (acetylene), 94.7 (acetylene), 127.9, 130.0, 131.5 (aromatic), 172.0 ($-COO-$).

p-(1-Nonynyl)benzoic Acid (7acid). The initial light yellow slurry was stirred under argon for 16 h at 80 °C. Yield 16.6479 g (70%) of 7acid. EA: Theory: 78.65% C, 8.25% H, 13.10% O; Actual: 78.40% C, 8.37% H. 300 MHz ^{1}H NMR ($CDCl_3$): $\delta = 0.88$ (t, 3 H, $-CH_3$), 1.3 (m, 8 H, $-CH_2-$), 1.6 (m, 2 H, $-CH_2-$), 2.4 (t, 2 H, $-CH_2-$), 7.4 (d, 2 H, aromatic), 8.0 (d, 2 H, aromatic).

p-(1-Decynyl)benzoic Acid (8acid). The initial light yellow slurry was stirred under argon for 46 h at 80 °C. Yield 7.0044 g (26.26%) of 8acid. EA: Theory: 79.03% C, 8.58% H, 12.39% O; Actual: 79.36% C, 8.73% H. 300 MHz ^{1}H NMR ($CDCl_3$): $\delta = 0.87$ (t, 3 H, −CH3), 1.4 (m, 10 H, $-CH_2-$), 1.6 (m, 2 H, $-CH_2-$), 2.4 (t, 2 H, $-CH_2-$), 7.4 (d, 2 H, aromatic), 8.0 (d, 2 H, aromatic). 75 MHz ^{13}C NMR ($CDCl_3$): $\delta = 14.1$ ($-CH_3$), 19.5 ($-CH_2-$), 22.7 ($-CH_2-$), 28.5 ($-CH_2-$), 28.9 ($-CH_2-$), 29.1 ($-CH_2-$), 29.2 ($-CH_2-$), 31.8 ($-CH_2-$), 80.1 (acetylene), 94.7 (acetylene), 127.9, 130.0, 131.5 (aromatic), 172.0 ($-COO-$).

6BP Monomer. To a heat/vacuum-dried and argon-flushed 500 mL three-neck flask with stir bar *p*-(1-octynyl)benzoic acid (8.95 g, 0.0389 mol) was added to benzene (60 mL) and stirred in an argon atmosphere. Oxalyl chloride (98%, 5.995 g, 8.9 mL, 0.047 mol) was slowly added with stirring. The solution was then heated to reflux. The bright yellow solution was stirred at reflux for 3.5 h and then allowed to cool to room temperature. The remaining benzene and oxalyl chloride were then removed via vacuum. The resulting *p*-(1-octynyl)benzoyl chloride was used immediately. Biphenol (1.3629 g, 0.0073 mol), diethyl ether (50 mL), and triethylamine (1.89 g, 2.6 mL, 0.019 mol) were stirred in an ice bath for 30 min. The freshly synthesized *p*-(1-octynyl)benzoyl chloride (4.6 mL, 0.0184 mol) was then slowly added. The slurry was then allowed to warm to room temperature and stir for 3.5 h. The volatiles were then removed via vacuum. Warm water (110 mL) was then added, and the resulting slurry was centrifuged and decanted. The solid was recrystallized from acetone and dried in a vacuum oven at 60 °C for 24 h to yield 4.4564 g (68%) of 6BP. EA: Theory: 82.59% C, 6.93% H, 10.48% O; Actual: 82.52% C, 7.18% H. 300 MHz ^{1}H NMR ($CDCl_3$): $\delta = 0.90$ (t, 6 H, $-CH_3$), 1.4 (m, 12 H, $-CH_2-$), 1.6 (m, 4 H, $-CH_2-$), 2.4 (t, 4 H, $-CH_2-$), 7.3 (d, 4 H, aromatic), 7.5 (d, 4 H, aromatic), 7.6 (d, 4 H, aromatic), 8.1 (d, 4 H, aromatic). 75 MHz ^{13}C NMR ($CDCl_3$): $\delta = 14.0$ ($-CH_3$), 19.6 ($-CH_2-$), 22.5 ($-CH_2-$), 28.5 ($-CH_2-$), 28.6 ($-CH_2-$), 31.3 ($-CH_2-$), 80.1 (acetylene), 94.7 (acetylene), 122.0, 128.0, 128.2, 129.8, 130.0, 131.6, 138.2, 150.4 (aromatic), 164.8 ($-COO-$).

3BP Monomer. Recrystallized from DMAC/water. EA: Theory: 82.11% C, 5.74% H, 12.15% O; Actual: 81.85% C, 5.51% H. 300 MHz ^{1}H NMR ($CDCl_3$): $\delta = 1.1$ (t, 6 H, $-CH_3$), 1.6 (m, 4 H, $-CH_2-$), 2.4 (m, 4 H, $-CH_2-$), 7.3 (d, 4 H, aromatic), 7.5 (d, 4 H, aromatic), 7.6 (d, 4 H, aromatic), 8.1 (d, 4 H, aromatic). 75 MHz ^{13}C NMR ($CDCl_3$): $\delta = 13.6$ ($-CH_3$), 21.5 ($-CH_2-$), 22.1 ($-CH_2-$), 80.2 (acetylene), 94.5 (acetylene), 122.0, 128.2, 129.7, 130.0, 131.6, 138.2, 150.4 (aromatic), 164.7 ($-COO-$).

4BP Monomer. Recrystallized from DMF/water. EA: Theory: 82.28% C, 6.18% H, 11.54% O; Actual: 82.61% C, 6.45% H. 300 MHz ^{1}H NMR ($CDCl_3$): $\delta = 0.96$ (t, 6 H, $-CH_3$), 1.5 (m, 8 H, $-CH_2-$), 2.4 (t, 4 H, $-CH_2-$), 7.3 (d, 4 H, aromatic), 7.5 (d, 4 H, aromatic), 7.6 (d, 4 H, aromatic), 8.1 (d, 4 H, aromatic). 75 MHz ^{13}C NMR ($CDCl_3$): $\delta = 13.6$ ($-CH_3$), 19.2 ($-CH_2-$), 22.0 ($-CH_2-$), 30.6 ($-CH_2-$), 80.1 (acetylene), 94.6 (acetylene), 122.0, 128.0, 128.2, 129.8, 130.0, 131.6, 138.2, 150.4 (aromatic), 164.7 ($-COO-$).

5BP Monomer. EA: Theory: 82.44% C, 6.57% H, 10.98% O; Actual: 82.29% C, 6.51% H. 300 MHz ^{1}H NMR ($CDCl_3$): δ = 0.93 (t, 6 H, $-CH_3$), 1.4 (m, 8 H, $-CH_2-$), 1.6 (m, 4 H, $-CH_2-$), 2.4 (t, 4 H, $-CH_2-$), 7.3 (d, 4 H, aromatic), 7.5 (d, 4 H, aromatic), 7.6 (d, 4 H, aromatic), 8.1 (d, 4 H, aromatic). 75 MHz ^{13}C NMR ($CDCl_3$): δ = 14.0 ($-CH_3$), 19.5 ($-CH_2-$), 22.2 ($-CH_2-$), 28.3 ($-CH_2-$), 31.1 ($-CH_2-$), 80.1 (acetylene), 94.7 (acetylene), 122.0, 128.1, 128.2, 129.8, 130.0, 131.6, 138.2, 150.4 (aromatic), 164.8 ($-COO-$).

7BP Monomer. EA: Theory: 82.72% C, 7.26% H, 10.02% O; Actual: 83.19% C, 7.30% H. 300 MHz ^{1}H NMR ($CDCl_3$): δ = .91 (t, 6 H, $-CH_3$), 1.3 (m, 12 H, $-CH_2-$), 1.5 (m, 4 H, $-CH_2-$), 1.6 (m, 4 H, $-CH_2-$), 2.4 (t, 4 H, $-CH_2-$), 7.3 (d, 4 H, aromatic), 7.5 (d, 4 H, aromatic), 7.6 (d, 4 H, aromatic), 8.1 (d, 4 H, aromatic). 75 MHz ^{13}C NMR ($CDCl_3$): δ = 14.1 ($-CH_3$), 19.6 ($-CH_2-$), 22.6 ($-CH_2-$), 28.6 ($-CH_2-$), 28.8 ($-CH_2-$), 28.9 ($-CH_2-$), 31.7 ($-CH_2-$), 80.1 (acetylene), 94.7 (acetylene), 122.0, 128.0, 128.2, 129.7, 130.0, 131.6, 138.2, 150.3 (aromatic), 164.8 ($-COO-$).

8BP Monomer. EA: Theory: 82.85% C, 7.56% H, 9.60% O; Actual: 82.82% C, 7.67% H. 300 MHz ^{1}H NMR ($CDCl_3$): δ = 0.88 (t, 6 H, $-CH_3$), 1.4 (m, 20 H, $-CH_2-$), 1.6 (m, 4 H, $-CH_2-$), 2.4 (t, 4 H, $-CH_2-$), 7.3 (d, 4 H, aromatic), 7.5 (d, 4 H, aromatic), 7.6 (d, 4 H, aromatic), 8.1 (d, 4 H, aromatic). [Due to low solubility, a carbon NMR was not recorded.]

Note: for the hydroquinone-derived monomers, the same procedure was followed; however, biphenol was replaced with the molar equivalent of hydroquinone, and the final monomer was recrystallized from DMF/water.

3HQ Monomer. EA: Theory: 79.98% C, 5.82% H, 14.21% O; Actual: 80.01% C, 5.92% H. 300 MHz ^{1}H NMR ($CDCl_3$): δ = 1.1 (t, 6 H, $-CH_3$), 1.6 (m, 4 H, $-CH_2-$), 2.4 (m, 4 H, $-CH_2-$), 7.2 (d, 4 H, aromatic), 7.5 (d, 4 H, aromatic), 7.6 (d, 4 H, aromatic), 8.1 (d, 4 H, aromatic). [Due to low solubility, a carbon NMR was not recorded.]

4HQ Monomer. EA: Theory: 80.31% C, 6.32% H, 13.37% O; Actual: 80.33% C, 6.63% H, 10.30% O. 300 MHz ^{1}H NMR ($CDCl_3$): δ = 0.95 (t, 6 H, $-CH_3$), 1.5 (m, 4 H, $-CH_2-$), 1.6 (m, 4 H, $-CH_2-$), 2.4 (t, 4 H, $-CH_2-$), 7.3 (d, 4 H, aromatic), 7.5 (d, 4 H, aromatic), 8.1 (d, 4 H, aromatic). 75 MHz ^{13}C NMR ($CDCl_3$): δ = 13.6 ($-CH_3$), 19.2 ($-CH_2-$), 22.0 ($-CH_2-$), 30.6 ($-CH_2-$), 80.1 (acetylene), 94.6 (acetylene), 122.6, 127.9, 129.8, 130.0, 131.6, 148.3 (aromatic), 164.6 ($-COO-$).

5HQ Monomer. EA: Theory: 80.60% C, 6.77% H, 12.63% O; Actual: 80.53% C, 7.0% H. 300 MHz ^{1}H NMR ($CDCl_3$): δ = 0.92 (t, 6 H, $-CH_3$), 1.4 (m, 8 H, $-CH_2-$), 1.6 (m, 4 H, $-CH_2-$), 2.4 (t, 4 H, $-CH_2-$), 7.3 (d, 4 H, aromatic), 7.5 (d, 4 H, aromatic), 8.1 (d, 4 H, aromatic). 75 MHz ^{13}C NMR ($CDCl_3$): δ = 14.0 ($-CH_3$), 19.5 ($-CH_2-$), 22.2 ($-CH_2-$), 28.3 ($-CH_2-$), 31.1 ($-CH_2-$), 80.1 (acetylene), 94.7 (acetylene), 122.6, 127.9, 129.8, 130.0, 131.6, 148.4 (aromatic), 164.6 ($-COO-$).

6HQ Monomer. EA: Theory: 80.56% C, 7.51% H, 11.92% O; Actual: 80.67% C, 7.35% H. 300 MHz ^{1}H NMR ($CDCl_3$): δ = 0.90 (t, 6 H, $-CH_3$), 1.4 (m, 12 H, $-CH_2-$), 1.6 (m, 4 H, $-CH_2-$), 2.4 (t, 4 H, $-CH_2-$), 7.3 (d, 4 H, aromatic), 7.5 (d, 4 H, aromatic), 8.1 (d, 4 H, aromatic). 75 MHz ^{13}C NMR ($CDCl_3$): δ = 14.1 ($-CH_3$), 19.6 ($-CH_2-$), 22.6 ($-CH_2-$), 28.5 ($-CH_2-$), 28.6 ($-CH_2-$), 31.3 ($-CH_2-$), 80.0 (acetylene), 94.7 (acetylene), 122.6, 127.9, 129.8, 130.0, 131.6, 148.3, (aromatic), 164.6 ($-COO-$).

7HQ Monomer. EA: Theory: 80.82% C, 7.85% H, 11.33% O; Actual: 81.60% C, 7.59% H, 10.30% O. 300 MHz ^{1}H NMR ($CDCl_3$): δ = 0.90 (t, 6 H, $-CH_3$), 1.3 (m, 12 H, $-CH_2-$), 1.4 (m, 4 H, $-CH_2-$), 1.6 (m, 4 H, $-CH_2-$), 2.4 (t, 4 H, $-CH_2-$), 7.3 (d, 4 H, aromatic), 7.5 (d, 4 H, aromatic), 8.1 (d, 4 H, aromatic). 75 MHz ^{13}C NMR ($CDCl_3$): δ = 14.1 ($-CH_3$), 19.6 ($-CH_2-$), 22.6 ($-CH_2-$), 28.6 ($-CH_2-$), 28.8 ($-CH_2-$), 28.9 ($-CH_2-$), 31.7 ($-CH_2-$), 80.0 (acetylene), 94.7 (acetylene), 122.6, 127.9, 129.8, 130.0, 131.6, 148.3, (aromatic), 164.6 ($-COO-$).

8HQ Monomer. EA: Theory: 81.32% C, 7.85% H, 10.83% O; Actual: 81.67% C, 8.12% H. 300 MHz ^{1}H NMR ($CDCl_3$): δ = 0.88 (t, 6 H, $-CH_3$), 1.4 (m, 20 H, $-CH_2-$), 1.6 (m, 4 H, $-CH_2-$), 2.4 (t, 4 H, $-CH_2-$), 7.3 (d, 4 H, aromatic), 7.5 (d, 4 H, aromatic), 8.1 (d, 4 H, aromatic). 75 MHz ^{13}C NMR ($CDCl_3$): δ = 14.1 ($-CH_3$), 19.5 ($-CH_2-$), 22.6 ($-CH_2-$), 28.5 ($-CH_2-$), 28.9 ($-CH_2-$), 29.1 ($-CH_2-$), 29.2 ($-CH_2-$), 31.8 ($-CH_2-$), 80.1 (acetylene), 94.7 (acetylene), 122.6, 128.0, 129.8, 130.0, 131.6, 148.3 (aromatic), 164.6 ($-COO-$).

Table 1. *n*HQ Series Transition Temperatures (in °C)

no. of carbons, *n*	crystal to smectic	crystal to nematic	smectic to nematic	nematic to isotropic
3		168		260
4		129		198
5		129		187
6		129		162
7		112		160
8	109		112	150

Table 2. *n*BP Series Transition Temperatures (°C)

no. of carbons, *n*	crystal to smectic	crystal to nematic	smectic to nematic	nematic to isotropic
3		204		365
4	193		211	335
5	172		214	327
6	155		219	306
7	152		228	292
8	149		226	287

Cross-Polarized Optical Microscopy (POM) of Isothermal Cures. POM experiments were conducted using a Nikon Fluorophot microscope (equipped with a video camera and recorder) and a Linkham Scientific Instruments HFS91 hot stage controlled by a TMS 91 temperature controller. Small amounts of the monomers were placed between two 12 mm round, glass microscope coverslips and observed between crossed polarizers. The sample was heated at a rate of 130 °C/min to the desired temperature and then held. The curing was recorded and allowed to continue until twice the time determined for the gelation time of the sample by parallel plate rheology. The liquid crystalline transition times and phases were determined by optical texture.

Thermal Analysis. Differential scanning calorimetry (DSC) was performed using a Seiko Instruments SSC5200 DSC220C with an SDM5600H data station. Samples of 5−10 mg were used. The heating rate used was 10 °C/min. The melting point and liquid crystalline transitions for the uncured monomers were determined from the extrapolated onsets of peaks in DSC experiments while in a nitrogen gas flow with a heating rate of 10 °C/min. All thermal transitions were confirmed during both heating and cooling using POM and are tabulated in Tables 1 and 2.

Gelation Determination via Parallel Plate Rheology. Gelation times were determined using a Paar Physica UDS 200, TC 10 temperature controller, and modified TEK 600 with parallel plate geometry. The sample chamber and 304-steel plates (a 25 mm diameter top plate and 50 mm diameter bottom plate) were preheated to the desired temperature for 60 min in a nitrogen atmosphere. A sample of approximately 0.15 g of monomer was loaded onto the lower plate. The upper plate was then lowered to form a gap of 0.25 mm. The sample was then tested with a 4% oscillating strain of 1 Hz frequency. The sample's gelation time was determined from the crossover point of the storage and loss moduli (tan δ = 1).

Results and Discussion

Effect of Molecular Architecture on Liquid Crystallinity. To observe the effects of molecular architecture on the liquid crystalline phases seen during isothermal curing, small samples of 3HQ, 3BP, 4BP, and 5BP were isothermally cured on a hot-stage equipped, cross-polarized optical microscope. The samples were observed for twice the time to gelation (as will be discussed in the following section) for each cure temperature. The 3HQ monomer was cured at 230, 240, 250, and 270 °C, while 3BP, 4BP, and 5BP were cured at

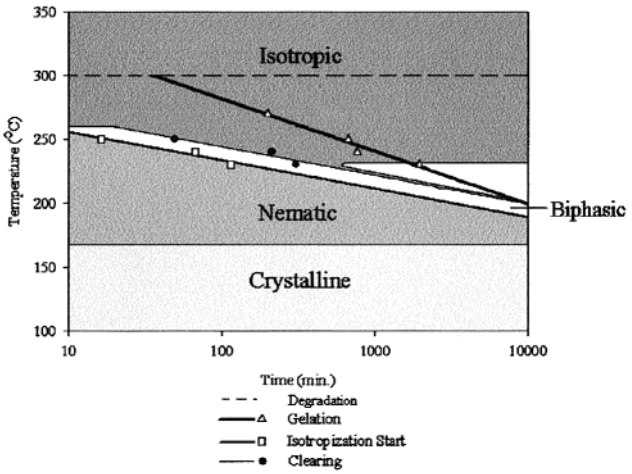

Figure 2. LCPTTT diagram of 3HQ.

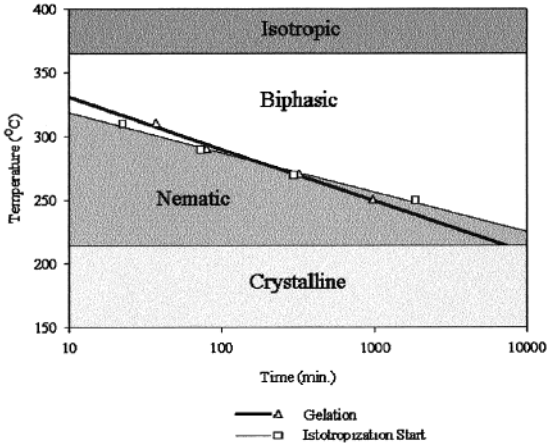

Figure 3. LCPTTT diagram of 3BP.

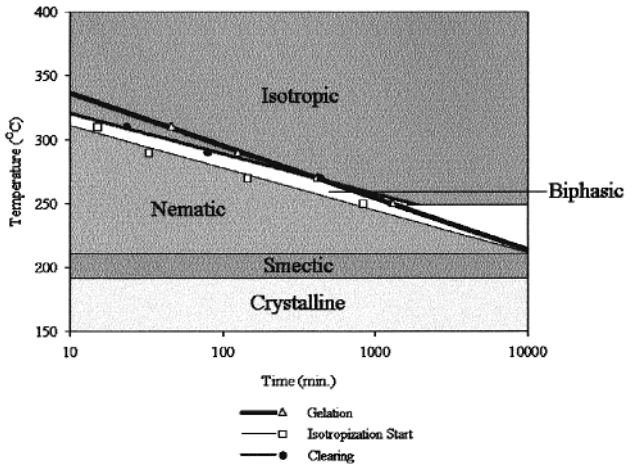

Figure 4. LCPTTT diagram of 4BP.

250, 270, 290, and 310 °C. Figures 2−5 are examples of the new liquid crystalline phase−time−temperature−physical transformation diagrams (LCPTTT) for 3HQ, 3BP, 4BP, and 5BP respectively, created to illustrate both physical and liquid crystalline transformations that occur during isothermal curing of these materials. The thick black line represents the time at which the material converts from a liquid to a gel for the isothermal cure temperature. The gel times have been fitted with exponential curves since the time to gelation is controlled by the reaction rate and should follow an Arrhenius relationship with the cure temperature. The

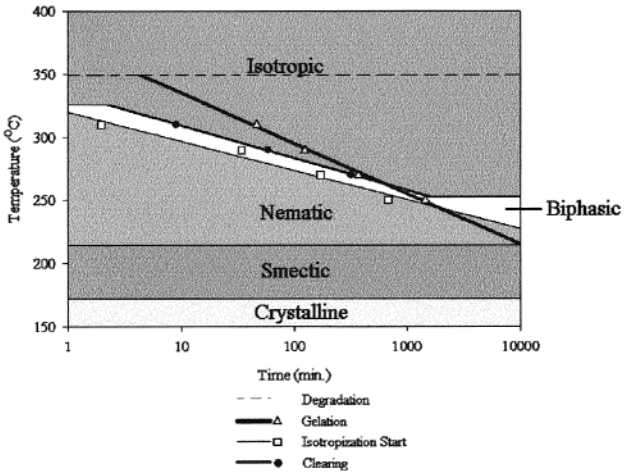

Figure 5. LCPTTT diagram of 5BP.

liquid crystalline phases are labeled and shaded. The melting, smectic to nematic transformation, and the clearing temperatures of the monomer are also illustrated in the diagrams. The liquid crystalline phase transition times (for the isotropization start times and final clearing times) have exponential curves similar to those for events following an Arrhenius relationship. There are four temperatures tested in each diagram. These points are fitted with exponential curves and extrapolated. The high-temperature end is below the degradation temperature of the monomer, while the low-temperature end is above the smectic and crystallization transition temperatures for the monomers. Since the area in which these curves are plotted should not have any additional confounding factors, the extrapolations should be valid.

As can be seen in all four of the diagrams, at the temperatures tested, these materials transform from an ordered nematic liquid crystal to either a biphasic nematic/isotropic or an isotropic material (except for 3HQ at 270 °C which starts in the isotropic phase). An example of the morphological development in 5BP isothermally cured at 310 °C progressing from the nematic phase to the isotropic phase is demonstrated in Figure 6. The micrographs were recorded from $t = 0$ to $t = 12$ min, where $t = 0$ is the time when the temperature reached 310 °C at 130 °C/min. The loss of liquid crystalline order is due to the lack of a spacer group between the polymer backbone and the mesogenic units. During polymerization, the molecular spacing between monomers changes to what is required for bond formation. If the new molecular distance is inconsistent with the spacing required for the liquid crystalline phase, a loss of liquid crystallinity will occur. Typically for side-chain LCPs, a flexible spacer group between the mesogenic unit and the backbone decouples the mesogen from the backbone, allowing more degrees of freedom while still maintaining the molecular ordering. Since in these monomers the reactive group is not decoupled from the mesogen, a loss of order during polymerization is not surprising. A similar, although smaller, effect has been seen in an off-lattice Monte Carlo simulation of network formation by rigid monomers.[25]

The retention of a biphasic structure (seen for all testing temperatures of 3BP and the lowest temperature for 4BP) is partially due to vitrification of the material, or ending of the testing period, before complete isotropization. The retention of a biphasic region for 5BP

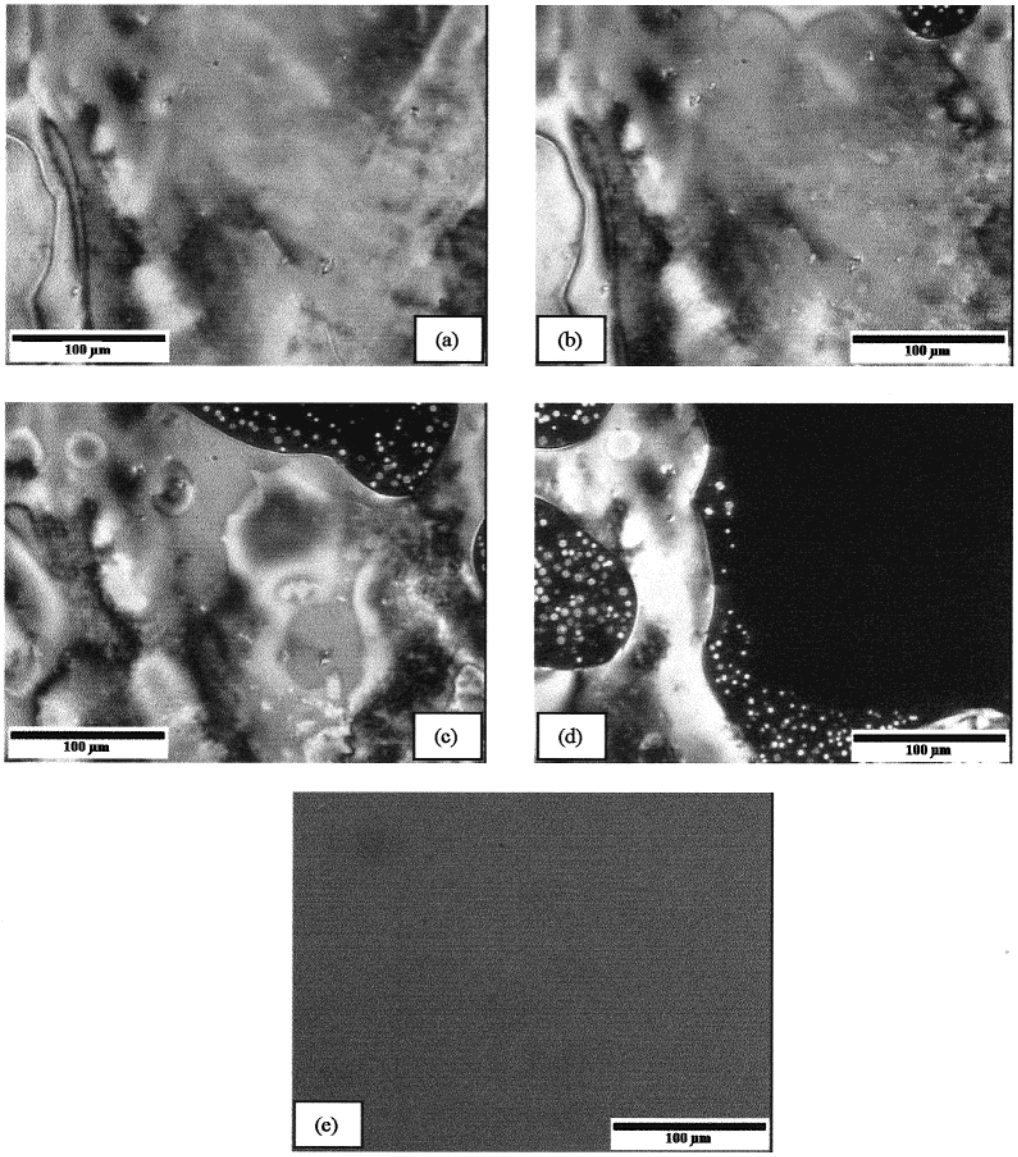

Figure 6. Series of polarized optical micrographs of 5BP progressing from nematic to isotropic as it is cured isothermally at 310 °C. Micrographs are taken at approximately (a) 10 s, (b) 2.5 min, (c) 3.5 min, (d) 6 min, and (e) 12 min after reaching 310 °C. Scale bar = 100 μm.

tested at 250 °C is different. In this case, toward the end of the transformation from nematic to isotropic, the material begins to reorder. It begins as pinpoint birefringent spots that grow and merge as curing continues. As seen in the LCPTTT diagram of Figure 2, for 3HQ at 230 °C, the material completely converts to an isotropic phase but regains some molecular ordering before vitrification. This is also illustrated in the micrographs of Figure 7. We have not been able to identify whether this phase is crystalline, smectic, or nematic. As the network grows, the reemergence of an ordered phase may be because of an increase in concentration of rigid rods per unit volume at higher conversions. This is similar to the reemergence, or initial emergence, of liquid crystalline phases seen for specific bis(acetylene)s,[3] bis(nadimide)s,[5] and liquid crystalline epoxies.[1,2] In those studies, the formation of liquid crystalline phases was attributed to an increase in axial ratio from chain extension. However, for the *n*BP and *n*HQ series the reordering often occurs after the three-dimensional network is already forming. In addition, the retention or re-formation of an ordered phase is only seen when the material is cured at lower temperatures. The temperature at which the ordered phase can appear decreases with increasing flexible chain length. This is due to a destabilization of liquid crystalline phases by the longer chains, thus lowering the clearing temperature.

Effect of Molecular Architecture on Gelation Times. The gelation times for the isothermal curing at 270 °C for the 12 monomers were determined using parallel plate rheology. The criterion for gelation was the crossover point between the G' and G'' curves. This is determined from when tan δ is equal to 1. Gel times were recorded as the last data point in which tan δ, the damping factor, was equal to 1. An example of the evolution of G', G'', and damping factor is shown in Figure 8. Figures 9 and 10 present the gel times for the *n*HQ and *n*BP series, respectively. The error bars for these plots (except for 4BP and 8BP) are the standard deviation from six runs of 3BP at 270 °C. For 4BP and 8BP, the error bars are the standard deviation from four runs of those monomers at 270 °C. The data point for 6BP has been excluded from Figure 10. When tested

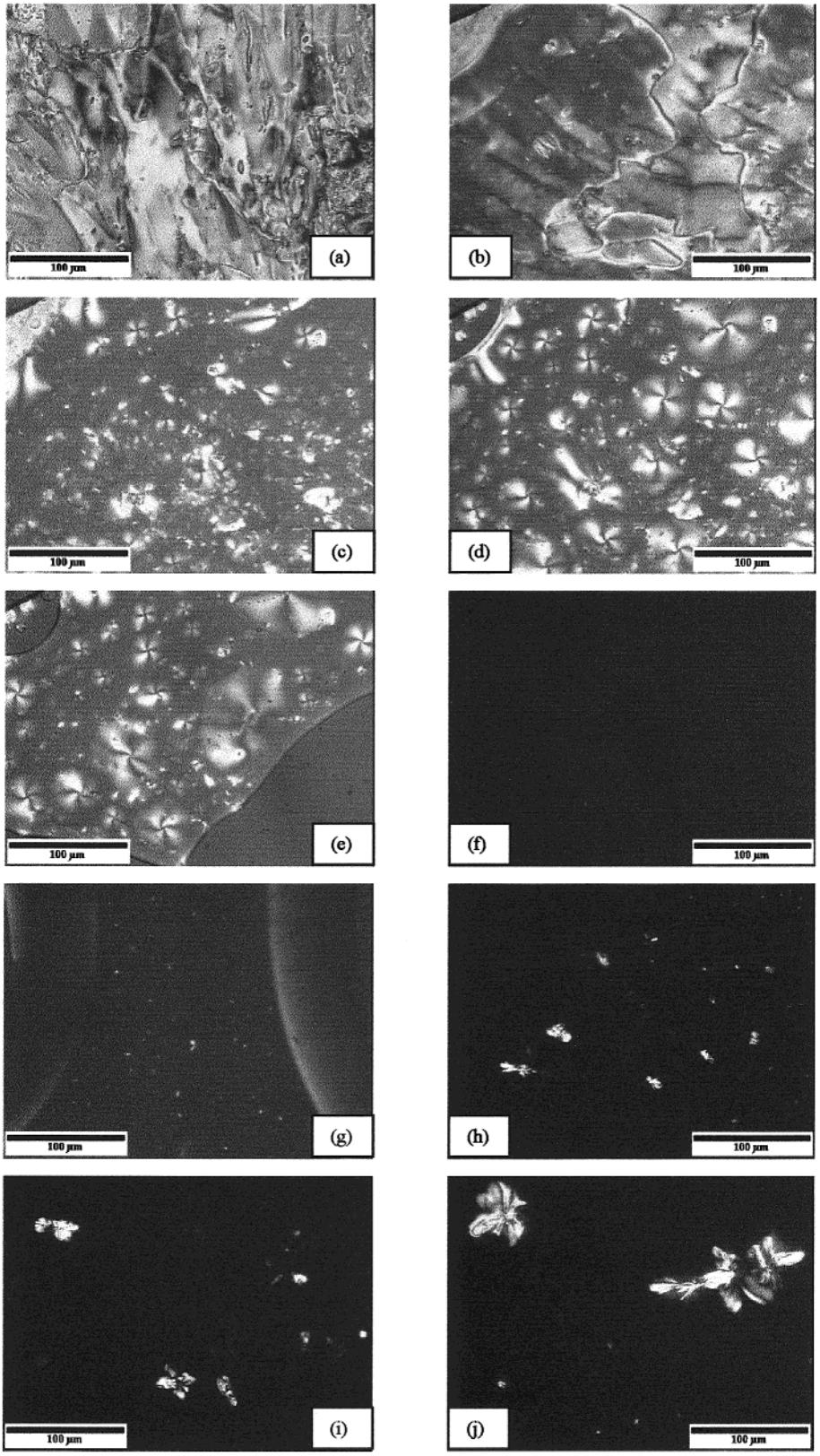

Figure 7. Series of optical micrographs of 3HQ as it is cured isothermally at 230 °C. Micrographs are taken at approximately (a) 1, (b) 70, (c) 80, (d) 170, (e) 200, (f) 530, (g) 880, (h) 1630, (i) 1700, and (j) 1980 min after reaching 230 °C. Scale bar = 100 μm.

multiple times, the time to gelation for 6BP ranged from 220 to 480 min, yielding an average value of 326 min with a standard deviation of about 111 min. The other monomers had a much smaller variability in their values with standard deviations ranging from 2 to 10 min. The large deviation measured for the 6BP sample is likely due to batch-to-batch differences in the amount of partial curing of the monomer during synthesis.

In previous studies of thermosetting systems,[14,17,18,26−30] it was determined that chemical conversion at the gel point is constant for a given reactive thermosetting system, independent of the time−temperature path

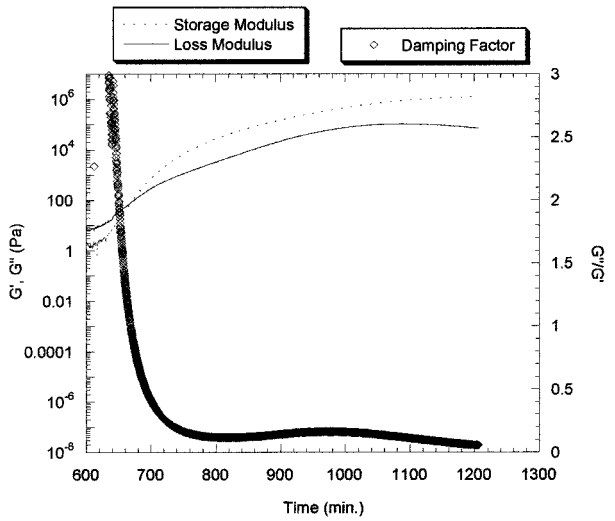

Figure 8. Rheological data for 3HQ while cured isothermally at 250 °C.

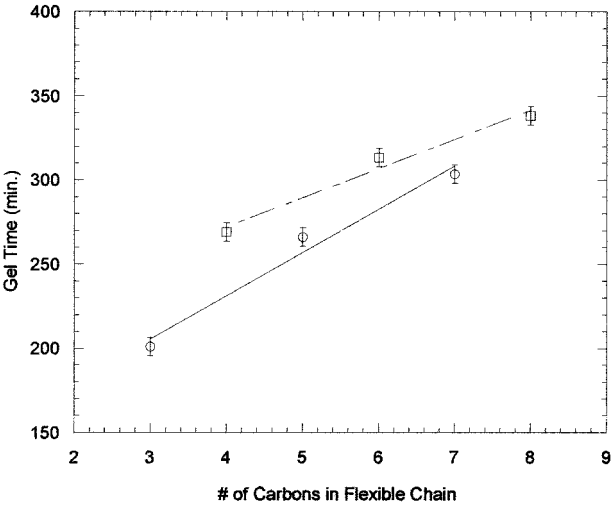

Figure 9. Plot of gel times for the *n*HQ series tested at 270 °C, 1 Hz, and 4% strain.

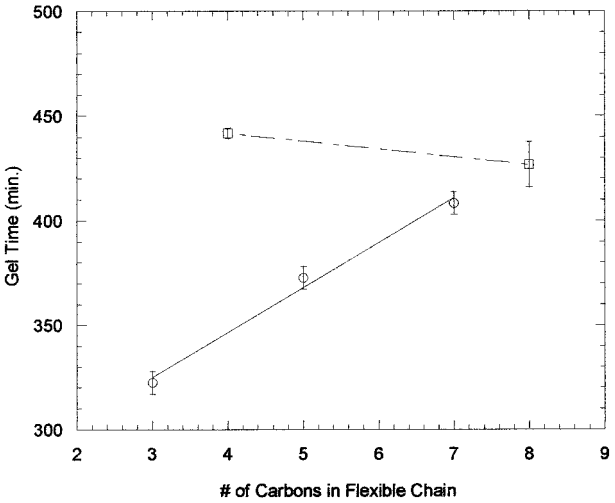

Figure 10. Plot of gel times for the *n*BP series tested at 270 °C, 1 Hz, and 4% strain.

taken. Initially it would be thought that as the flexible chain length linearly increases, the gel time would also linearly increase due to a rise in steric hindrance. As seen in Figures 9 and 10, there is an increase in the time to gelation with increasing chain length; however, the increase is not linear. Rather, an odd−even effect is seen for the gel times of both series. This is especially surprising for the *n*HQ series due to the fact that the monomers are isotropic at this temperature, as previously reported. The lack of order would seem to discount the traditional explanation of end group interactions being responsible for the occurrence of odd−even effects in this case.[31] However, while the macroscopic isotropy of the material was confirmed from POM experiments, we believe that the monomers may have localized molecular alignment due to their rigid molecular structure. Therefore, the traditional explanation of end group interactions causing an odd−even effect may still be valid.

Comparison of the gel times for monomers with equal length but different central mesogenic units, 3HQ and 3BP for example, shows that the monomers with the shorter mesogen reach gelation more quickly. This may be due to an increase in molecular mobility available to the smaller, more flexible monomer or a higher reactivity of its acetylene groups.

As seen in Figure 10, the gel times of the *n*BP series also do not increase monotonically with increasing chain length, also indicating a possible odd−even effect. In addition, although the *n*HQ monomers with even chain lengths show a significant increase in gel time when the chain length increases from four to eight carbons, in the *n*BP series an increase from four to eight carbons results in almost no change in gel time. This lack of significant change in gel time with increasing chain length implies independence for the cure rate with respect to the chain length for chains of even carbon length. Also of note is that, for both series, the odd and even curves for the gel times seem to be converging at around $n = 8$. This is similar to the trend seen for the clearing temperatures of the monomers. The convergence implies that the differences in cure kinetics between chains of odd and even length decrease with increasing chain length and might even disappear with chains of a critical length.

Conclusions

The effects of molecular architecture on the liquid crystalline phases and times to gelation for two series of acetylene functionalized LCT monomers were studied. The monomers could be cured at temperatures between 230 and 310 °C. Through the use of a rheometer with parallel plate geometry, a hot stage, and a cross-polarized optical microscope the new liquid crystalline phase−time−temperature−physical transformation diagrams (LCPTTT) were constructed for four of the monomers. These diagrams illustrate that the monomers change from nematic liquids to isotropic or biphasic gels during isothermal curing. However, reemergence of an ordered phase occurred if the monomers were cured at low enough temperature. The critical temperature for ordered phase retention in the final vitrified material is inversely proportional to the length of the flexible chain. This may be due to a destabilization of the liquid crystalline phases with increasing chain length. Also, as expected from the characterization of the monomers, the *n*BP series had greater liquid crystalline phase stability during isothermal curing than the *n*HQ series.

The gel times for the two series of monomers were compared for isothermal cures of 270 °C. It was shown that monomers of the *n*HQ series reached gelation more

quickly than the monomers of the *n*BP series with the same flexible chain length. This is attributed to a decrease in molecular mobility with increasing mesogenic unit length. Both series did show an increase in gel times with increasing chain length; however, the increase was not in a linear manner as expected. Instead, an odd−even effect was seen in both series, even though the *n*HQ series was cured in the isotropic phase at 270 °C. This is especially surprising since traditional reasoning for this effect requires the molecules to begin in an ordered state prior to the transition to enable significant interaction between molecular end groups. However, in this study the molecules may be maintaining localized molecular alignment that cannot be observed by POM. Also surprising was the fact that the data for the molecules with even flexible lengths for the *n*BP series did not increase significantly with increasing chain length. This shows an enhancement or leveling of the cure rate with increasing chain length, at least for chains of even length. The gel times for both series also appeared to be converging at around $n = 8$, thus indicating the loss of the odd−even effect for monomers with chains of greater length. This is similar to the convergence seen for the clearing temperatures of the monomers.

Acknowledgment. This work was supported by the U.S. Army Research Office under Grant DAAG55-98-1-0114 to Dr. Elliot P. Douglas as a Presidential Early Career Award for Scientists and Engineers.

References and Notes

(1) Lin, Q.; Yee, A. F.; Earls, J. D.; Hefner, R. E. J.; Sue, H.-J. *Polymer* **1994**, *35*, 2679.
(2) Carfagna, C.; Amendola, E.; Giamberini, M. *Liquid Crystalline Epoxy Resins*; Carfagna, C., Ed.; Pergamon Press: Oxford, UK, 1994; pp 69−85.
(3) Douglas, E. P.; Langlois, D. A.; Benicewicz, B. C. *Chem. Mater.* **1994**, *6*, 1925.
(4) Shiota, A.; Körner, H.; Ober, C. K. *Macromol. Chem. Phys.* **1997**, *198*, 2957.
(5) Hoyt, A. E.; Benicewicz, B. C. *J. Polym. Sci., Part A: Polym. Chem.* **1990**, *28*, 3417.
(6) Domszy, R. C.; Shannon, P. J. *Macromolecules* **1990**, *23*, 2790.
(7) Cadenato, A.; Salla, X. R. J. M.; Morancho, J. M.; Marroyo, L. M.; Martin, J. L. *J. Therm. Anal.* **1997**, *49*, 269.
(8) Tatsumiya, S.; Yokokawa, K.; Miki, K. *J. Therm. Anal.* **1997**, *49*, 123.
(9) Hong, M. S.; Chung, I. J. *Polym. J.* **1991**, *23*, 747.
(10) DeMeuse, M. T.; Gillham, J. K.; Parodi, F. *J. Appl. Polym. Sci.* **1997**, *64*, 15.
(11) Gillham, J. K.; Enns, J. B. *TRIP* **1994**, *2*, 406.
(12) Simon, S. L.; Gillham, J. K. Annual Technical Conference-ANTEC 94, Conference Proceedings Pt. 2, 1994; p 2192.
(13) Simon, S. L.; Gillham, J. K. *J. Appl. Polym. Sci.* **1992**, *46*, 1245.
(14) Enns, J. B.; Gillham, J. K. *J. Appl. Polym. Sci.* **1983**, *28*, 2567.
(15) Langlois, D. A.; Benicewicz, B. C.; Douglas, E. P. *Chem. Mater.* **1998**, *10*, 3393.
(16) Mallon, J. J.; Adams, P. M. *J. Polym. Sci., Part A: Polym. Chem.* **1993**, *31*, 2249.
(17) Heise, M. S.; Martin, G. C.; Gotro, J. T. *Polym. Eng. Sci.* **1990**, *30*, 83.
(18) Laza, J. M.; Julian, C. A.; Larrauri, E.; Rodriguez, M.; Leon, L. M. *Polymer* **1998**, *40*, 35.
(19) Harran, D.; Laudouard, A. *J. Appl. Polym. Sci.* **1986**, *32*, 6043.
(20) Izuka, A.; Winter, H. H.; Hashimoto, T. *Macromolecules* **1997**, *30*, 6158.
(21) Jahromi, S.; Kuipers, W. A. G.; Norder, B.; Mijs, W. J. *Macromolecules* **1995**, *28*, 2201.
(22) Sastri, S. B.; Keller, T. M.; Jones, K. M.; Armistead, J. P. *Macromolecules* **1993**, *26*, 6171.
(23) Hergenrother, P. M.; Smith, J. G. J. *Polymer* **1994**, *35*, 4857.
(24) Bucca, D.; Keller, T. M. *J. Polym. Sci., Part A: Polym. Chem.* **1997**, *35*, 1033.
(25) Kurdikar, D. L.; Boots, H. M. J.; Peppas, N. A. *Macromolecules* **1995**, *28*, 563210.
(26) Wisanrakkit, G.; Gillham, J. K. *J. Appl. Polym. Sci.* **1991**, *42*, 2453.
(27) Gillham, J. K. *Polym. Eng. Sci.* **1979**, *19*, 676.
(28) Wisanrakkit, G.; Gillham, J. K. *J. Appl. Polym. Sci.* **1990**, *41*, 2885.
(29) Wisanrakkit, G.; Gillham, J. K. *J. Coating Technol.* **1990**, *62*, 35.
(30) Gillham, J. K.; Benci, J. A.; Noshay, A. *J. Polym. Sci.* **1974**, *46*, 279.
(31) Boese, R.; Weiss, H.-C.; Blaser, D. *Angew. Chem., Int. Ed.* **1999**, *38*, 988.

MA001884+